INVESTIGATION OF THE COLUMNAR-TO-EQUIAXED TRANSITION DURING SOLIDIFICATION OF A TRANSPARENT ALLOY USING A TEXUS MODULE

Gerhard Zimmermann[(1)], Laszlo Sturz[(1)], Burkhard Schmitz[(2)], Irmin Meyer[(2)]

[(11]ACCESS e.V., Intzestrasse 5, 52072 Aachen, Germany, Email: G.Zimmermann@access-technology.de
[(2)]Astrium GmbH, Space Transportation, Airbus-Alle 1, 28199 Bremen, Germany

ABSTRACT

The columnar to equiaxed transition (CET) during solidification is of great importance, because the resulting microstructure determines the materials properties. Investigating the dynamics of CET a transparent alloy solidifying like metals is selected, which allows the in-situ observation of columnar and equiaxed growth by use of optical diagnostics. To suppress convective melt flow during solidification and to avoid sedimentation of growing equiaxed grains in the melt an experiment in microgravity environment is prepared for the TEXUS 47 sounding rocket mission. Besides the description of the flight hardware scientific results of preparatory test experiments on ground are presented.

1. INTRODUCTION

In casting of metallic alloys a transition from a columnar solidification structure to an equiaxed one often is observed. This columnar-to-equiaxed transition (CET) is of high technological relevance, since the material properties are related strongly to the microstructures. CET is directly associated with the existence of equiaxed grains in the melt ahead of the columnar growing front. For the CET the columnar growth front needs to be arrested by such equiaxed grains, either by mechanical [1] or solutal blocking [2]. The level of understanding of CET is summarized in [3], whereas very recently a comparison of different CET prediction methods is given in [4].

To achieve a more fundamental understanding of CET two different approaches are made: First, microgravity environment allows process conditions without buoyancy effect. Therefore, equiaxed grains will grow in the undercooled melt in-place, showing neither sedimentation nor transport due to thermo-solutal convection. Solidification experiments performed in the sounding rocket mission MAXUS-7 using AlSi7 alloys clearly demonstrate that CET occurs earlier in microgravity environment than on earth [5]. Second, using in-situ observation methods the dynamics of formation and growth of equiaxed grains can be observed directly. Such an approach exists for AlCu and AlNi alloys using synchrotron radiation. That way CET can be investigated in sheet-like samples in-situ and in real-time [6, 7].

Solidification under reduced gravity with in-situ diagnostics can be realized by using transparent alloys and optical observation methods. During the sounding rocket missions TEXUS 36 and 40 the morphological instability in directional solidification of succinonitrile-acetone alloys was investigated successfully using video observation [8]. In this paper the preparatory work is presented, which is necessary for in-situ investigation of CET in a transparent alloy during the coming TEXUS 47 mission.

2. EXPERIMENTAL SET-UP

To realize solidification experiments in a sounding rocket mission a specific module for TEXUS was built by Astrium GmbH. Based on module TEM 06-23, which was successfully flown in two previous TEXUS missions [8], especially the experiment chamber and the optical diagnostics were modified and adapted to the scientific requirements.

Figure 1 shows a sketch of the experimental set-up. The frame of the chamber was made from stainless steel, covered by two quartz glass plates of 4 mm thickness. Between these windows a sheet-like sample with 16 mm height, 20 mm width and 1 mm depth was placed. The frame is equipped with filling holes and connected to a volume compensation reservoir. The solidification within the experiment chamber will be performed by using the gradient-freeze technique which allows a simple optical access and a furnace design without moving components. Therefore the chamber is equipped with a heater at the top and a Peltier element as cooler at the bottom side. The heater and cooler temperatures are independently controlled to realize proper temperature gradients and cooling rates for the solidification experiment. To monitor the temperature field inside the sample, 5 thermocouples are inserted from the side through the frame at equidistant vertical positions every 2.5 mm. The sheet-like sample is illuminated with quasi-parallel light from the backside, which is emitted by an array of LED and collimated by an optical system.

The solidification structure is observed optically with two CCD cameras using a beam splitter. One of the

Proc. '19th ESA Symposium on European Rocket and Balloon Programmes and Related Research, Bad Reichenhall, Germany, 7–11 June 2009 (ESA SP-671, September 2009)

cameras is used to take overview pictures and to control the complete growth process. In the optical path to the other camera a long-distance microscope allows to observe a field of view of 2.1 x 1.7 mm² in a zoom mode. Both microscope and camera are mounted on a table, which allows movement in horizontal and vertical direction as well as focussing through the depth of the sample. That way the sections relevant for investigation of CET can be selected during the experiment run via telecommand. A photograph of the complete module TEM 06-23 is shown in Fig. 2.

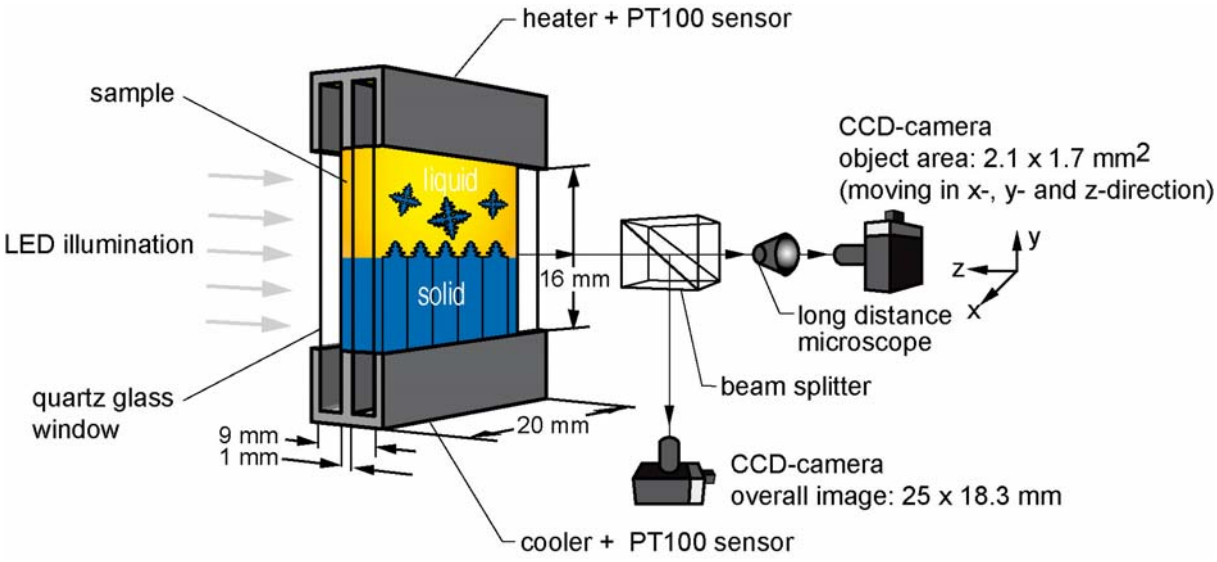

Figure 1. Sketch of the experiment chamber and the optical system

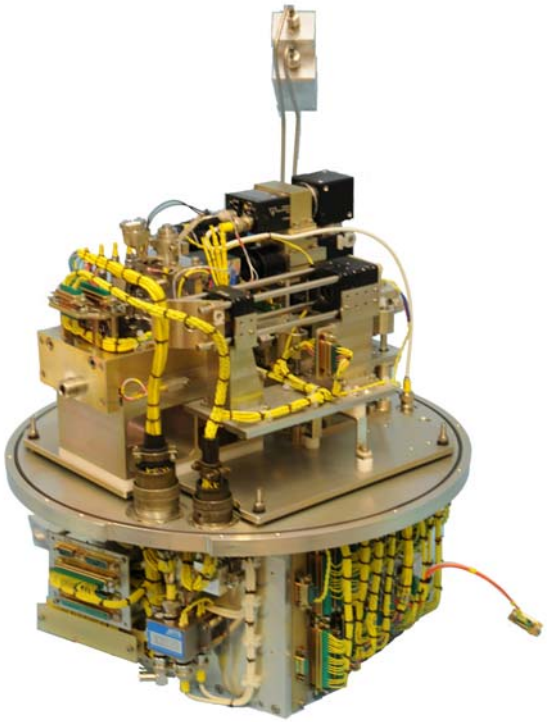

Figure 2. Modified TEXUS module TEM 06-23(Astrium GmbH)

3. EXPERIMENT PARAMETER

3.1. Alloy system

Organic alloys to be used for in-situ observation has to solidify like metals, i.e. in a non-facetted way. Additionally a columnar-to-equiaxed transition must exist in an accessible parameter range. Therefore the binary system neopentylglycol-(D)camphor is selected. The phase diagram given in Fig. 3 shows an eutectic point at 36.2 mol% or 45 wt% (D)camphor and at a temperature of 53°C [9].

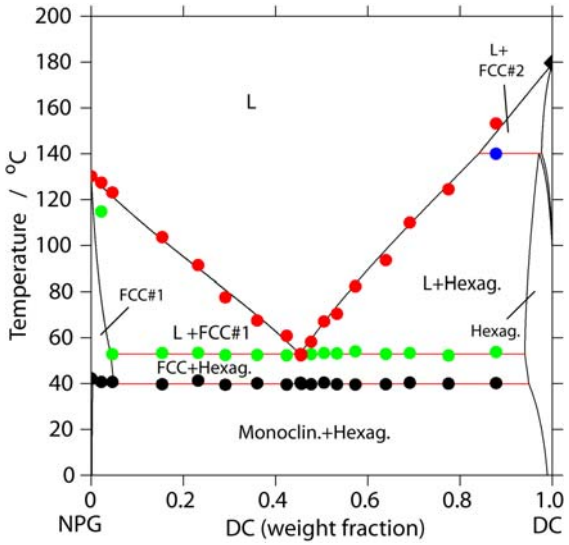

Figure 3. Phase diagram neopentylglycol-(D)camphor

For CET investigations alloy compositions between 30 and 40 wt% (D)camphor will be used, because of their lower temperature and higher probability for CET compared to diluted alloys. For these hypoeutectic compositions neopentylglycol will solidify as primary dendritic phase. The sample materials for the experiments was alloyed from neopentylglycol and (D)camphor, which has been purified by sublimation in Ar-atmosphere in a glovebox to purities of about 99.95%.

3.2. Experiment sequence

A typical experiment sequence consists of several steps. In the first step the alloy material is completely melted. A thermal mixing of the melt for about 1 hour allows solutal homogenization of the alloy. Then, a temperature gradient along the sample is established by setting the heater and cooler temperatures to about 90° C and 45° C, respectively. Directional solidification of neopentylglycol-(D)camphor from bottom to top is initiated by applying constant cooling rates at the heater and the cooler of typically 0.28 K/min. After columnar growth for about 5 mm the cooling rates are increased to 2 K/min to trigger CET.

4. EXPERIMENTAL RESULTS

CET is mainly determined by the temperature gradient and the velocity of the solid-liquid interface. Therefore these parameters have to be measured. For numerical modeling of CET also the nucleation number density is important. This chapter describes how these parameters can be evaluated from the experiment.

4.1. Temperature gradient

Fig. 4 shows the temperature profiles of a representative test experiment. At time t = 1260 s the cooling rates of heater and cooler are increased from 0.28 K/min to 2 K/min. The resulting thermal behaviour inside the sample measured by the thermocouples T1 to T5 is also given in Fig. 4. Calculated from these temperature measurements the mean value of the temperature gradient in the alloy is about 1.8 K/mm (Fig. 5).
The offset in G results from slightly non-equidistant positions of the thermocouples. The raise of G(T4-T5) after increasing the cooling rate is correlated to directional solidification from bottom, i.e. to a slightly lower heat conductivity of solid phase compared to the melt [10]. Additionally, release of latent heat may be taken into account which affects locally the temperature gradient.

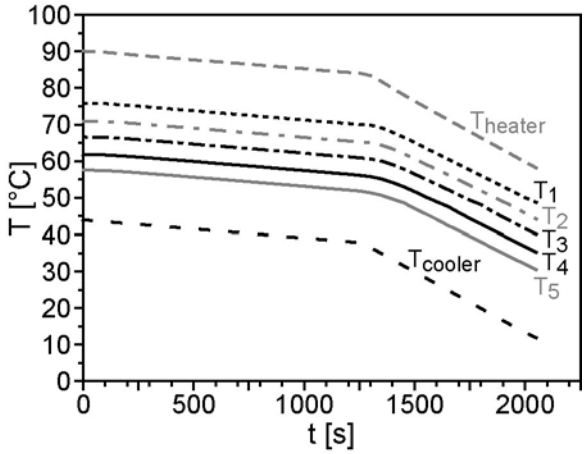

Figure 4. Heater and cooler temperatures and temperature profiles inside the sample (T1 to T5)

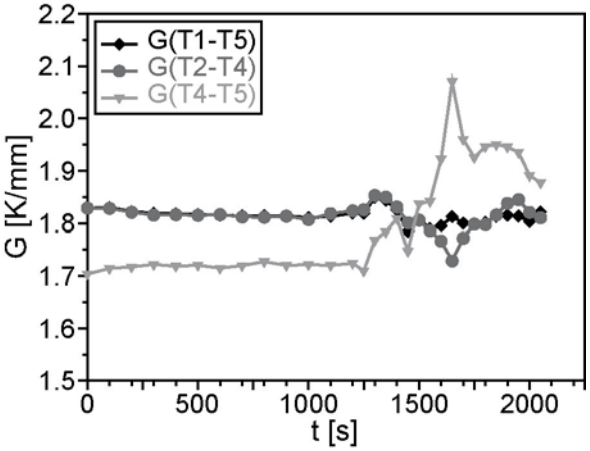

Figure 5. Temperature gradients calculated from temperatures given in Fig.4

4.2. Growth velocity

The local velocity of the columnar solid-liquid interface is determined from the macroscopic video film. Therefore single images are extracted. Digital image analysis like median filtering and segmentation is used to smoothen the dendritic structure. Then the position of the macroscopic solidification front can be identified automatically by setting a grey level threshold. For illustration Fig. 6 shows vertical lines in a macroscopic image ranging from the top to the s/l interface.
Six of such contact points marking the positions of the moving front are given in Figs. 7 and 8.
The differences in the pixel positions result in a slighly curved macroscopic solid-liquid interface and in the dendritic interface morphology itself. But the general behaviour needed to determine the interface velocity is unitary. From Fig. 7 it can be seen that there is a transient period of several minutes until steady state growth for cooling rate 0.28 K/min is esatblished. Converting with a pixel size of 28.3 µm from the

measured gradient a macroscopic interface velocity of v_1 = 1.9 µm/s is found. Fig. 8 gives in more detail the interface movement while increasing the cooling rate to 2 K/min at time t = 1260 s. Using the same evaluation technique the interface velocity increase from of v_1 = 1.9 µm/s to v_2 = 5.2 µm/s.

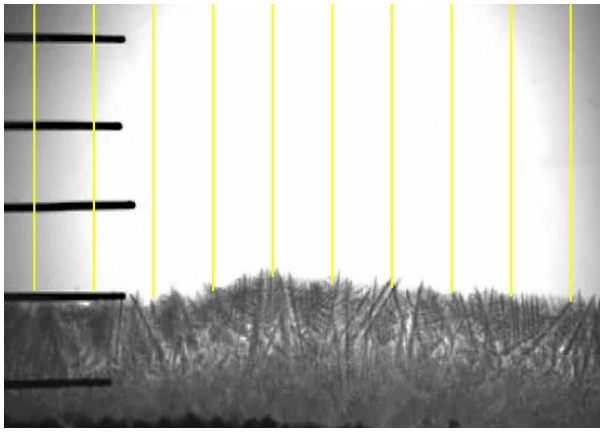

Figure 6. Macroscopic image to determine the interface velocity at different lateral position

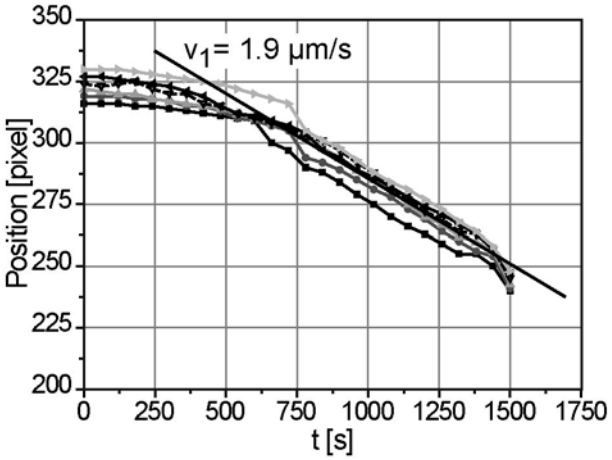

Figure 7. Solid/iquid interface positions evaluated from macro images for the cooling rate 0.28 K/min

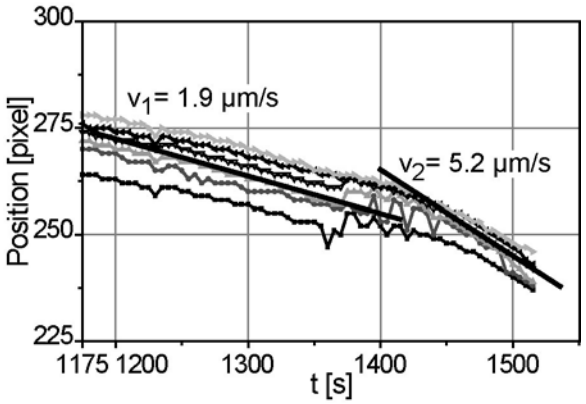

Figure 8. Solid/liquid interface positions evaluated from macro images while increasing the cooling rate

From the images recorded with the microscope and CCD optics details of the solidification structure can be resolved. In Figs. 9 and 10 two images of columnar growing dendrites are shown, taken at t = 300 s and t = 1000 s, respectively.

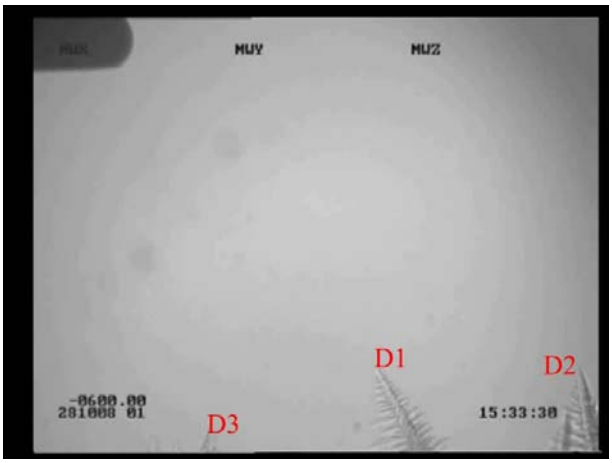

Figure 9. Detail image showing the growth of single dendrites at t = 300 s

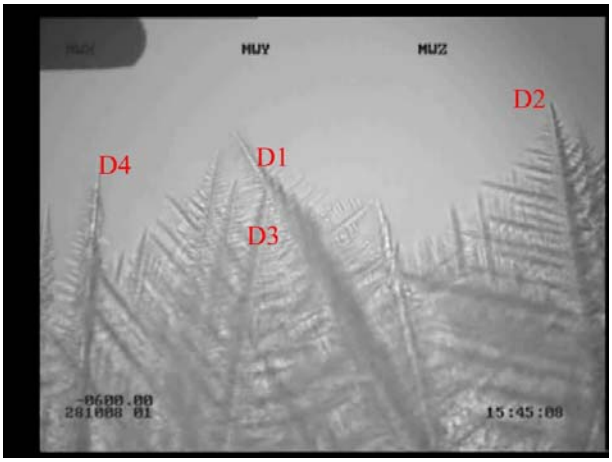

Figure 10. Detail image showing the same field of view as in Fig. 9 at t = 1000 s

To determine the local growth velocity 4 dendrite tips are marked and tracked. In Fig. 11 the tracks of dendrites D1, D2 and D4 are shown. Dendrite D3 was not accounted for, because it was overgrown by dendrite D1 (see Fig. 10). The marking of dendrite D4 was started later at t = 635 s. From these tracks in the time interval between t = 800 s and t = 1000 s, and using a converting factor of 1 pixel = 2.73 µm for the micro image, the local growth velocities of dendrites D1, D2 and D4 are 1.60 µm/s, 1.71 µm/s and 1.65 µm/s. This corresponds well to the front movement take from the macro images (see Figs. 6 and 7).

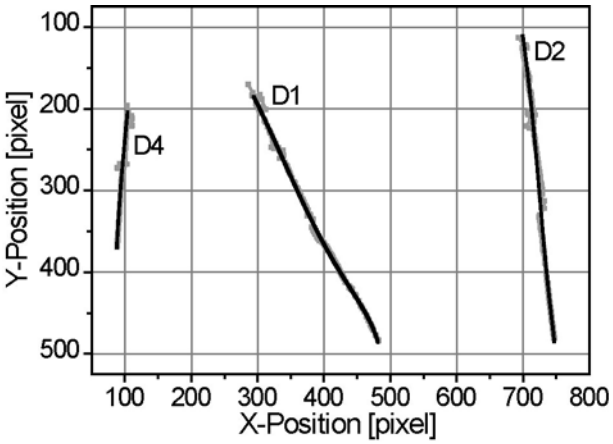

Figure 11. Tracks of 3 columnar growing dendrites

4.3. Nucleation number density

At critical values of the temperature gradient G_c and the interface velocity v_c the nucleation of equiaxed grains in the undercooled melt is initiated. Fig. 12, taken at t = 1450 s, shows the nucleation of the first two grains (marked by circles). Following that more and more grains start nucleating and growing. For example such a situation is given in Fig. 13 for t = 1541 s. Additionally, a more detailed analysis of the position of the equiaxed grains can be obtained from the micro images.

Evaluating the critical values G_c and v_c for CET and the nucleation number density numerical models can be used to determine the nucleation undercooling. With it a prediction of CET for other parameter sets will be feasible.

Figure 12. Nucleation of two equiaxed grains (marked by circles) in the undercooled melt at t = 1450 s

Figure 13. Many growing equiaxed grains ahead of the columnar solid-liquid interface at t = 1541 s

4.4. Gravitational effect

Especially the growth of equiaxed grains in the undercooled melt is influenced by gravitational effect. Due to different densities of solid grains and liquid, sedimentation of the the grains may occur. Additionally, on earth bouyancy convection may transport the nuclei due to convective motion. An example is shown in Fig. 14.

The micro images demonstrate the evolution of two equiaxed grains with time. The dendrite arms of both grains grow significantly. Moreover the upper right dendrite moves downwards and closer to the second grain. Simulateously a rotation of this equiaxed dendrite is observed. Therefore, it's obvious that CET is affected by gravity.

For validation of numerical modelling well-defined, diffusive boundary conditions are required. Therefore, an experiment in microgravity environment during the TEXUS 47 mission will be performed.

5. CONCLUSION

Based on preparatory experiments on ground it is demonstrated that columnar-to-equiaxed transition (CET) in a transparent alloy can be observed in-situ by optical means. Tests were performed in the TEXUS flight hardware TEM 06-23, which is developped and manufactored by Astrium Space Transpartation GmbH in Bremen. Using power down technique the set-up allows columnar growth of neopentylglycol-(D)camphor alloy as well as a transition to equiaxed growth of dendrites while increasing the cooling rate. Video observations is made with two CCD cameras, one showing the whole process chamber and the other

one showing just a detail. From such images the averaged velocity of the moving solid-liquid interface and the local growth velocities of single dendrites is determined. The temperature profile in the samples is measured by 5 thermocouples. With it the critical values at CET for the temperature gradient and the interface velocity are determined. Also, from these images the positions and number of growing nuclei in the undercooled melt is evaluated.

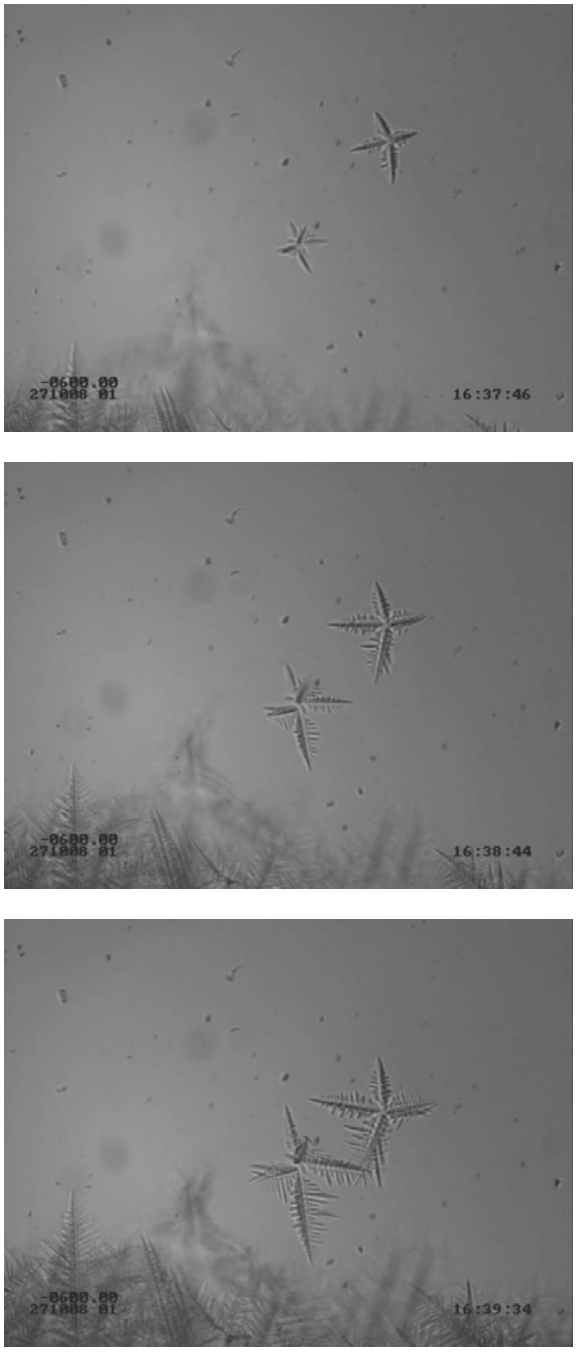

Figure 14. Growth and movement of equiaxed grains in gravity; time intervals between successive images Δt = 58 s and Δt = 50 s; field of view 2.1 x 1.7 mm²

In the flight hardware, additionally the microscopic CCD camera will be movable in a defined window. This enlarges the field of view and allows the detection of a larger number of equiaxed grains.
Besides these scientific evaluations it was demonstrated that the experimental set-up will allow CET investigation within a sounding rocket mission. The selection of a proper alloy concentration and adapted process parameters may allow to trigger CET within 6 minutes of microgravity time. Such an experiment, investigating CET in-situ and in a diffusive region, will be performed in fall 2009 during the TEXUS 47 campaign.

6. ACKNOWLEDGEMENTS

This work was financially supported by the German Space Agency DLR, which is gratefully acknowledged. The authors appreciate the Team of Astrium Space Transportation GmbH in Trauen for the hardware development and support during the preparatory experiments.

7. REFERENCES

1. Hunt J.D. (1984). *Mat. Sci. Eng.* **65**, 75-83.
2. Martorano M.A., Beckermann C. & Gandin Ch.-A. (2003). *Met. Mat. Trans*. **34A**, 1657-1674.
3. Spittle J.A. (2006). *Int. Materials. Rev.* **51**, 247-269.
4. McFadden S., Browne D.J. & Gandin Ch.-A. (2009). *Met. Mat. Trans.* **40A**, 662-672.
5. Sturz L., Zimmermann G., Jung H., Mangelinck-Noel N., Nguyen-Thi H. & Billia B. (2007). *ESA SP* **647**, 367-372.
6. Mathiesen R.H., Arnberg L., Bleuet P. & Somogyi A. (2006). *Met. Mat. Trans.* **37A**, 2515-2524.
7. Nguyen-Thi H., Reinhart G., Mangelinck-Noel N., Jung H., Billia B., Schenk T., Gastaldi J., Haertwig J. & Baruchel J. (2007). *Met. Mat. Trans.* **38A**, 1458-1464.
8. Weiss A. & Zimmermann G. (2003). *ESA SP* **530**, 101-106.
9. Witusiewicz V.T., Sturz L., Hecht U. & Rex S. (2004). *Acta Materialia* **52**, 5519-5527.
10. Ocak Y., Akbulut S., Keslioglu K. & Marasli N. (2008). *J. Colloid and Interface Science* **320**, 555-562.